Probing lattice dynamics of $Cd_2Re_2O_7$ pyrochlore: Thermal transport and thermodynamics study

J. He,* D. Hitchcock, I. Bredeson, N. Hickman, Terry M. Tritt, and S. N. Zhang
118 Kinard Physics Laboratory, Department of Physics and Astronomy, Clemson University, Clemson, South Carolina 29634, USA
(Received 24 February 2010; published 7 April 2010)

$Cd_2Re_2O_7$ single crystals exhibit an amorphouslike lattice thermal conductivity, κ_{latt}. At temperatures about twice the Debye temperature, the phonon mean-free path approaches the value of the average Cd-Cd spacing while the specific heat is at values notably lower than the classical Dulong-Petit limit. We show that a model that treats Cd ions as Einstein oscillators embedded in a Debye host with strong optical-acoustic phonon coupling and some very high-frequency optical phonon modes in the system, can account for these features. Despite no structural change, κ_{latt} undergoes a smooth slope change at ~340 K, above which the resistivity adopts a weak power-law behavior. The combined results of resistivity, thermopower, specific-heat, thermal-conductivity, and Hall coefficient measurements corroborate that a phonon-mediated electron-hole scattering mechanism sets in above room temperature.

DOI: 10.1103/PhysRevB.81.134302 PACS number(s): 63.20.−e, 72.15.Eb, 65.40.Ba, 72.10.−d

I. INTRODUCTION

The discovery of superconductivity in $Cd_2Re_2O_7$,[1–3] the first among the pyrochlore oxides, led to a revived interest in its normal-state properties.[4,5] While the superconductivity turned out to be of a Bardeen-Cooper-Schrieffer type-II,[6,7] the normal state $Cd_2Re_2O_7$ is intriguing in its own right. It features a moderately correlated Fermi-liquid state right above the superconductivity transition at $T_c \sim 1.0$ K,[2] a weak changeover at $T' \sim 120$ K that lacks a signature in thermodynamics and is possibly imperfection driven,[8,9] as well as a metal-to-better metal second-order phase transition at $T^*=200$ K that is accompanied by a cubic-to-tetragonal structure change.[10,11] Concomitant with the marked change in the resistivity, thermopower, magnetic susceptibility, specific heat, and Hall coefficient are the subtle lattice symmetry evolution and exceptionally small lattice constant displacement across and below T^*.[8–17]

The lattice dynamics associated with the cubic-to-tetragonal phase transition at $T^*=200$ K has proved extraordinary. The order parameter of the transition involves a Brillouin-zone centered, doubly degenerate optical phonon mode of E_u symmetry.[12] Below T^*, softening of this E_u mode leads to two distinct but nearly degenerate crystal structures ($I4_122$ and $I\bar{4}m2$) with an infinitesimal anisotropy gap in the excitation spectrum. The long wavelength fluctuations between these two structures give rise to the exotic "Goldstone-mode" phonon dynamics.[13,18] At temperatures well above the anisotropy scale, the Goldstone mode is predicted to have a linear dispersion relation near the Brillouin-zone center in all directions.[13] Mapping the detailed phonon-dispersion relation by inelastic neutron scattering is desired but the experiment was complicated for the strong resonating absorption effects of ^{114}Cd.[19]

Above T^*, $Cd_2Re_2O_7$ adopts a pyrochlore lattice with space group $Fd\bar{3}m$. Figure 1 illustrates a pyrochlore lattice of generic stoichiometry $Cd_2Re_2O_6O'$, with oxygen anions occupying O(48*f*) and O′(8*b*) sites, respectively.[20] The aforementioned E_u mode is dominated by the collective displacement of O(48*f*) anions.[13] It is well known that the pyrochlore compounds often have low-frequency optical phonon modes that are ready to couple with the heat-carrying acoustic phonon.[20] From the crystallography point of view, the "underbonded" Cd ions reside in the oversized hexagonal channel voids formed by six rigid ReO_6 octahedra, which could give rise to some dynamic or static disorder.[16,21,22] The Raman spectroscopy study has identified a population of optical modes with wave numbers less than ~100 cm^{-1}, in addition to some very high-frequency optical modes.[21,22] How these peculiar lattice features affect the thermodynamics and thermal transport properties of $Cd_2Re_2O_7$ is largely unexplored.

Note also that a very limited number of experimental works have been performed in the range above room temperature,[11,23] there has been little effort devoted to understanding how the high-temperature physical properties derive from the pyrochlore lattice. For instance, the resistivity of $Cd_2Re_2O_7$ slowly increases from ~445 $\mu\Omega$ cm at $T^*=200$ K to ~485 $\mu\Omega$ cm at 600 K due to some strong scattering but it shows no sign of saturation.[11] It is reminiscent of the "bad-metal" behavior.[24] As similar features have been observed in other itinerant pyrochlore systems, such as $Cd_2Os_2O_7$,[25] $Nd_2Mo_2O_7$,[26] and $Bi_2Ru_2O_7$,[27] irrespective of their distinct ground states, it raises an interesting possibility that the scattering mechanism is specific to the pyrochlore lattice. Moreover, the high-temperature resistivity of $Cd_2Re_2O_7$ is found to be nonlinear in temperature,[11] whereas a linear temperature dependence is expected from the

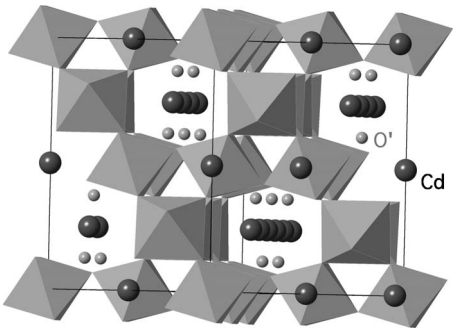

FIG. 1. Illustration of the pyrochlore structure of $Cd_2Re_2O_6O'$.

 ©2010 The American Physical Society

electron-phonon coupling usually dominant at temperatures comparable to the Debye temperature ($\theta_D \sim 397$ K[10]).[28]

Therefore a combined specific-heat and thermal-conductivity study is essential for understanding the lattice dynamics of $Cd_2Re_2O_7$. Until now, however, there has been no report on the thermal conductivity; the previous specific-heat study was mainly focused on the range below room temperature. In this paper, we report a study of thermal conductivity up to 720 K and specific heat up to 820 K in single crystal of $Cd_2Re_2O_7$. Supplanted by the results of the resistivity, thermopower, and Hall coefficient measurements, it not only gives us insight into the lattice dynamics of $Cd_2Re_2O_7$ but also helps understand the interplay between the charge and lattice degrees of freedom in a wide range above room temperature. The features of the lattice dynamics obtained in this study should have some exemplary characteristics for the wide class of pyrochlore oxides of generic stoichiometry 2-2-7.

II. EXPERIMENTAL METHODS

Large single crystals of $Cd_2Re_2O_7$ were grown using a vapor transport technique[16] and cut into appropriate shapes with dimension of a few mm^3 for various characterizations. The resistivity (2–720 K), thermopower/Seebeck coefficient (5–720 K) and thermal conductivity (5–310 K) were measured on a Quantum Design® Physical Properties Measurement System (PPMS) and our custom-made apparatuses[29,30] using a four-probe steady-state technique. The possibility of reversible oxygen loss/gain above room temperature has been ruled out by performing the consecutive resistivity and thermopower measurements in vacuum and 1/3 atmosphere of Ar. The specific heat above room temperature (319–820 K) was measured on a Netzsch® 404c high-temperature differential scanning calorimeter (below 308 K on the PPMS). The thermal conductivity κ above room temperature was calculated using the formula $\kappa=\rho_m C_v D$, where ρ_m is the mass density, C_v the specific heat per unit volume, and D the thermal diffusivity that was measured on a Netzsch® LFA457 laser flash system. The Hall coefficient measurement (5–330 K) was preformed on the PPMS using a five-probe configuration with the magnetic field sweeping between ± 3.0 T at each temperature. As the crystal structure is practically isotropic in the temperature range studied,[17] there was no attempt to measure transport properties along specific crystallographic directions.

III. RESULTS AND DISCUSSIONS

A. Semimetallic normal state

Shown in the main panel of Fig. 2 are the resistivity, ρ, measured from 2 to 720 K and the thermopower, α, from 5 to 720 K. The normal-state resistivity exhibits an overall metallic character with distinct temperature dependences in different temperature regimes. Closer examination identified two power-law-featured regimes: namely, (a) 2 K$<T<$60 K and (b) 330 K$<T<$650 K. While the quadratic temperature dependence in regime (a) is a signature of the electron-electron interaction in a Fermi-liquid state,[2] the origin of the

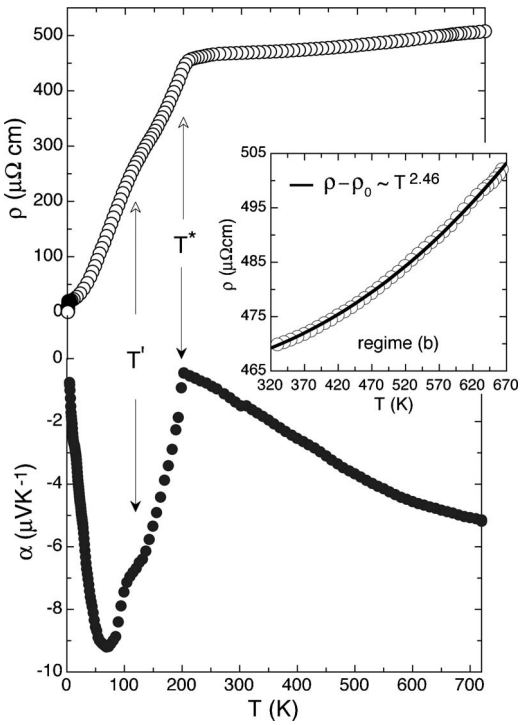

FIG. 2. Main panel: temperature dependences of the resistivity ρ and the absolute thermopower α. Inset: a power-law resistivity behavior $\rho-\rho_0 \sim T^p$ is identified between 330 and 650 K, namely, in the regime (b).

power-law behavior in regime (b) is not clear. The resistivity behavior in the regime (b) is well described by a power-law behavior $\rho-\rho_0=AT^p$ with $\rho_0=463\pm1$ $\mu\Omega$ cm and p $=2.5\pm0.1$ (inset of Fig. 2). The wide temperature range of measurement is essential for extracting the power-law component out of the small variation in $(\rho-\rho_0)$. It is also noted that the resistivity does not show any sign of saturation up to 720 K. Unlike resistivity, the thermopower is sensitive to the Fermi-surface topology.[31] In a metal the thermopower is usually dominated by the diffusive term, α_D, linear in temperature, as expressed in the Mott's formula[24]

$$\alpha_D \sim \frac{\pi^2 k_B^2 T}{3e}\left(\frac{\partial \ln \sigma}{\partial \varepsilon}\right)_{\varepsilon=E_F}, \quad (1)$$

where σ is the electrical conductivity when Fermi energy $E_F=\varepsilon$, e the electron charge and k_B the Boltzmann's constant. We note that α changes almost linearly with temperature in the regime (a) whereas it exhibits a stretched "S" shape above T^*, suggesting a semimetal-like band structure above T^*.

In Fig. 3 we present the temperature variations in Hall coefficient, R_H, and Hall mobility, $\mu_H=(R_H/\rho)$, from 5 to 330 K. Below T', R_H is nearly temperature independent while μ_H follows a $T^{-3/2}$ behavior down to ~40 K, consistent with a dominant phonon-scattering mechanism in a metal with a weakly temperature-dependent carrier concentration. In the vicinity of T^*, α, R_H, and μ_H are strongly temperature dependent and they vary cooperatively, indicating a band-structure rearrangement. The band-structure cal-

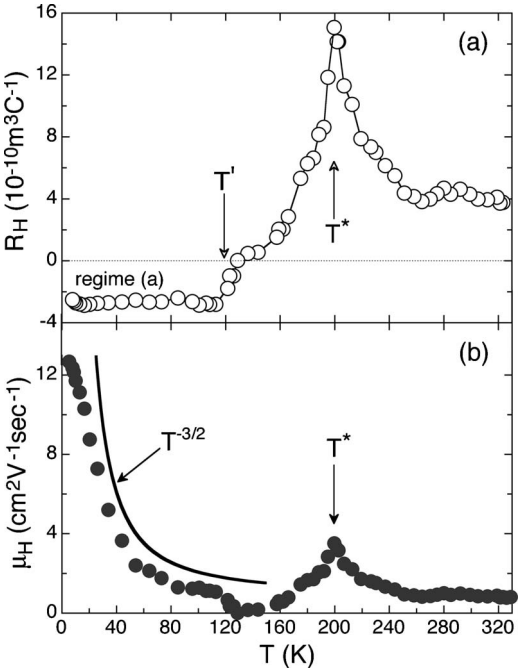

FIG. 3. Temperature dependences of (a) Hall coefficient, R_H and (b) Hall mobility, μ_H.

culations characterized $Cd_2Re_2O_7$ as a compensated semimetal with a Fermi surface consisting of light electron pockets at the Brillouin-zone center and heavy hole sections near the zone boundaries.[32] As is shown in Fig. 3(a), R_H changes sign near T', and R_H and α have opposite signs above T'. In this context, the small but strongly temperature-dependent α is likely due to the partial cancellation of the electron and hole contributions. If the magnitude of α can be treated as a measure of the degree of such cancellation, there should be a larger electron-hole cancellation above T^*, which precludes a simple one-band analysis of the resistivity and thermal conductivity in regime (b). Above 250 K, both R_H and μ_H are nearly temperature independent. The small magnitude of μ_H is a reflection of the close values of the electron and hole mobilities.[33]

The associated temperature variations in the resistivity, thermopower, Hall coefficient, and Hall mobility constitute sufficient evidence for a metallic normal state that is essentially governed by the band structure. Besides, the system is paramagnetic in the temperature range studied.[34] Coupled with the results of the band-structure calculations, it is inferred that the heavy holes are the leading carrier and they strongly scatter the light electrons above T^*. The phase transition at T^* and the changeover at T' successively remove a substantial portion of the hole band from the Fermi surface. As a result, the loss of density of states leads to a higher electrical conductivity below T^* and the electrons finally become the leading carrier below T'. The electron-hole scattering mechanism will be invoked in Sec. III in order to explain the electrical and thermal conduction behavior in regime (b).

B. Thermal conductivity and specific heat

We now proceed to the thermal conductivity κ of $Cd_2Re_2O_7$ that should have two heat-carrying entities, electron and phonon. In the simplest scheme, we have $\kappa = \kappa_{Latt} + \kappa_e$, where κ_{Latt} and κ_e are the lattice and carrier thermal conductivity, respectively. The Wiedemann-Franz (W-F) relation yields $\kappa_e = \sigma T L_0$, where σ is the electrical conductivity and L_0 the Lorenz number, 2.44×10^{-8} $W\Omega/K^2$.[35] It should be mentioned that the simultaneous electron and hole conduction in regime (b) leads to an additional term from the bipolar thermal-diffusion effect,[36] the κ_{Latt} derived from the W-F relation is somewhat overestimated. We present κ, κ_{Latt}, and κ_e from 5 to 720 K in Fig. 4. The observed κ resembles that of the polycrystalline, isostructural $Cd_2Os_2O_7$.[25]

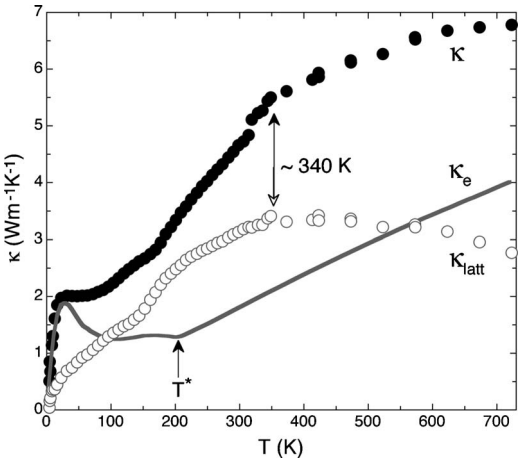

FIG. 4. Temperature dependences of total thermal conductivity, κ, electron thermal conductivity, κ_e, and lattice thermal conductivity, κ_{latt}. The arrow denotes the kink in κ_e due to the phase transition at T^*.

The lattice thermal conductivity of a crystalline material usually peaks at a temperature of a few tenths of θ_D and follows a T^{-1} dependence at elevated temperatures due to the Umklapp phonon-phonon interaction.[36] Despite the well-proved single-crystalline nature, the $Cd_2Re_2O_7$ specimen exhibits a largely amorphouslike κ_{latt}: small in magnitude and $d\kappa_{latt}/dT \geq 0$ over a wide temperature regime. There is no discernable feature in the vicinity of T^*, consistent with the predominantly electronic nature of the phase transition at T^*. The other interesting finding is that both κ and κ_{latt} undergo a slope change at ~340 K, which lacks a signature in the specific heat, resistivity, and thermopower. The origin of this slope change will be addressed in Sec. III.

1. Optical-acoustic phonon coupling

Crystalline materials may exhibit amorphouslike lattice thermal conductivity when the optical-acoustic phonon coupling dominates the thermal transport. This often occurs in materials having a unit cell with a large number of atoms.[36,37] $Cd_2Re_2O_7$ has 88 atoms in one unit cell and the Raman spectroscopy study revealed a population of low-frequency optical modes.[21,22] Concerning the thermal transport, the coupling between the low-frequency optical bands and the long wavelength heat-carrying acoustic bands results in less band dispersion and therefore less heat-carrying capability. On the other hand, the presence of low-frequency optical modes is expected to cause a deviation in the low-

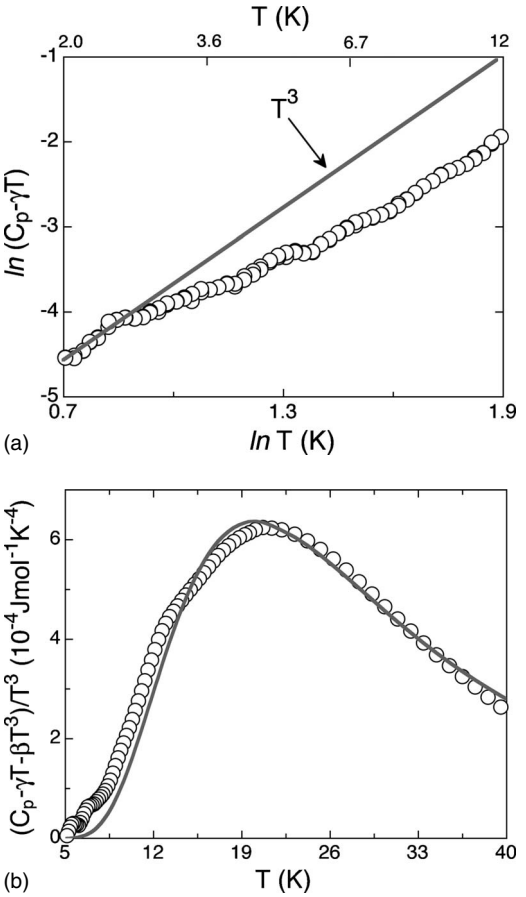

FIG. 5. (a) The plot of $(C_p-\gamma T)$ vs T deviates from the Debye T^3 fashion (solid line) below 5 K. (b) the plot of $(C_p-\gamma T-\beta T^3)/T^3$ vs T reveals a hump feature centered at ~20 K, which is well described by an Einstein oscillator mode with $\theta_E \sim 98$ K (solid line).

temperature specific heat from the classical Debye model that only takes into account long wavelength acoustic phonon modes.

2. Einstein oscillators in a Debye host

The Debye model of lattice vibration is in general too simple but it should be adequately precise at temperatures below $(\theta_D/50)$, where only long wavelength acoustic phonon modes are excited and contribute a T^3 term in the specific heat. In $Cd_2Re_2O_7$, $(\theta_D/50) \sim 8$ K. Fitting the isobaric specific heat C_p between 1.8 and 5 K into the formula $C_p=\gamma T+\beta T^3$ yields $\gamma=29.8$ mJ mol^{-1} K^{-2} and $\beta=0.317$ mJ mol^{-1} K^{-4}, where γ and β are the coefficients of the electronic and lattice specific heat, respectively. As is shown in Fig. 5(a), $(C_p-\gamma T)$ vs T clearly deviates from the Debye T^3 fashion below 5 K, indicating excitations other than the long wavelength acoustic modes. Furthermore, the plot of $(C_p-\gamma T-\beta T^3)/T^3$ vs T in Fig. 5(b) reveals a hump feature centered at ~20 K. This hump feature is hard to interpret within the Debye model but it can be readily described by the Einstein oscillator

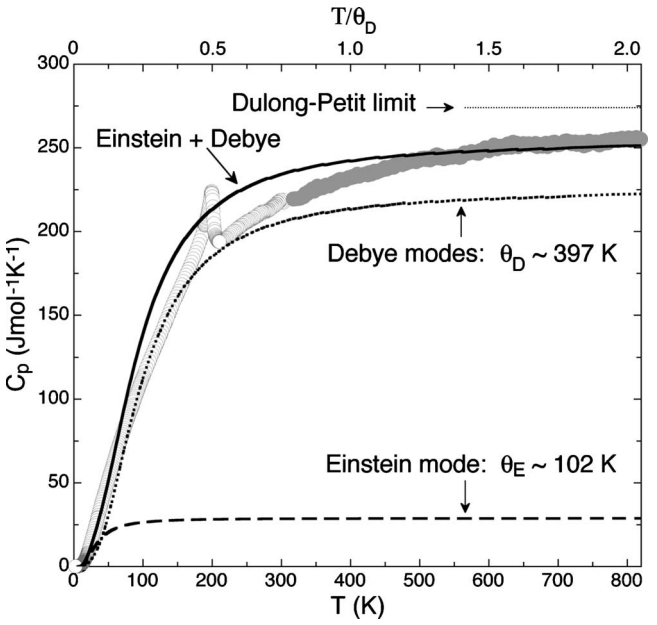

FIG. 6. The low temperature and high temperature parts of specific heat C_p are well approximated by the scenario of "an Einstein mode in a Debye host."

$$C_p^E = Z\frac{\left(\frac{\theta_E}{T}\right)^2 e^{\theta_E/T}}{(e^{\theta_E/T}-1)^2} \tag{2}$$

with an Einstein temperature $\theta_E \sim 98$ K and the vibration strength $Z=28.9$ J mol^{-1} K^{-1}. Note that the θ_E of a localized oscillator can be independently determined from the mean-square-displacement amplitude U_{iso} via the formula

$$U_{iso} = \frac{\hbar^2 \coth(\theta_E/2T)}{2mk_B\theta_E}, \tag{3}$$

where m is the reduced mass and k_B the Boltzmann's constant.[38] The room temperature value $U_{iso} \sim 0.0125$ Å^2 yields $\theta_E \sim 102$ K for the Cd ions.[16] Therefore, in conjunction with the crystallography consideration, the Cd ions have been identified as the entity of the Einstein oscillators.

Of interest is that the value of $Z=28.9$ J mol^{-1} K^{-1} is considerably lower than the $6R=49.88$ J mol^{-1} K^{-1} ($R=8.314$ J mol^{-1} K^{-1}), the value expected for two Einstein oscillators (Cd ions) per molecule. Meanwhile, C_p reaches ~93% of the classical Dulong-Petit limit at 820 K (Fig. 6).[39] Valuewise, the deficit in Z from $6R$ is close to the C_p deficit from the Dulong-Petit limit. Figure 6 clearly shows that the low-temperature part (5–40 K) and high-temperature part (500–820 K) of C_p are well approximated by the formula

$$C_p = Z\frac{\left(\frac{\theta_E}{T}\right)^2 e^{\theta_E/T}}{(e^{\theta_E/T}-1)^2} + 3R(2+7)\int_0^{\theta_D}\frac{x^4e^x}{(e^x-1)^2}dx. \tag{4}$$

There are no adjustable parameters in Eq. (4). There are several possible explanations for the C_p deficit from the Dulong-Petit limit. Apart from the anharmonicity (e.g., phonon-phonon interactions),[40,41] one possible explanation is the

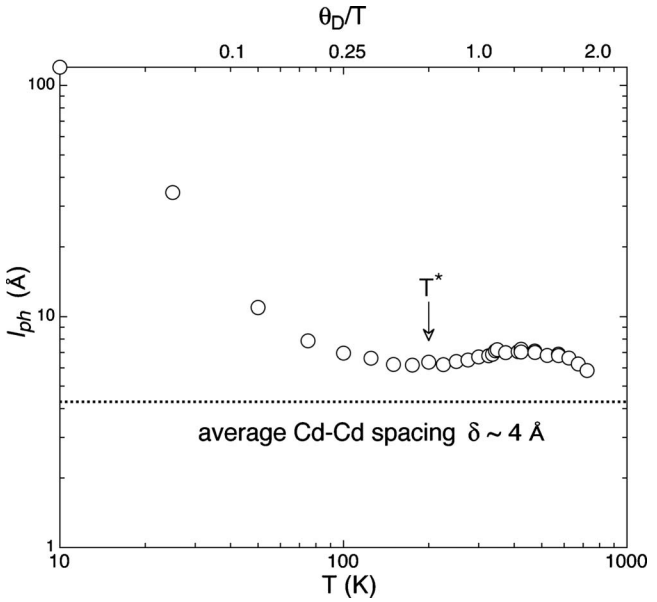

FIG. 7. The phonon mean free path, l_{ph}, is shown, along with the value of average Cd-Cd distance, δ.

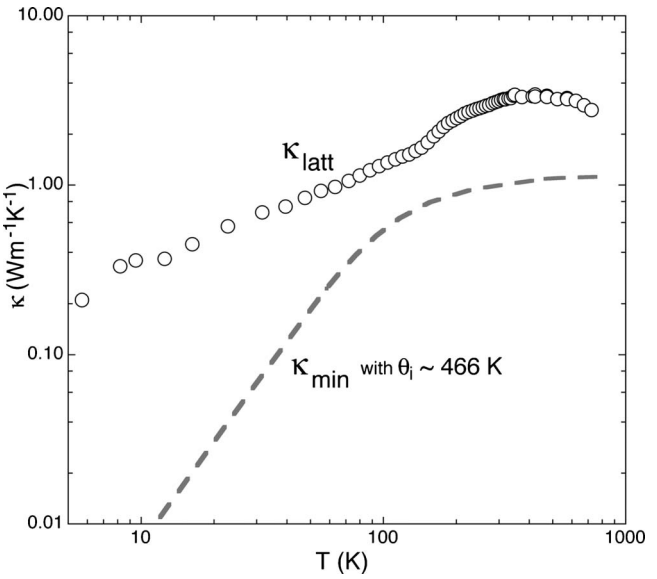

FIG. 8. The lattice thermal conductivity, κ_{latt}, (open circle) is compared with the calculated amorphous lattice thermal conductivity, κ_{min}, as described in the text (solid line).

presence of some very high-frequency phonon modes[21,22] that "freezes out" at suitably low temperatures.[41,42] Indeed, the Raman spectroscopy measurement revealed some phonon modes with frequencies that exceed ~650 cm^{-1} (energetically ~910 K).[21,22] The other possibility worth further investigation is that the Cd sublattice behaves like liquid at elevated temperatures.

3. Phonon mean-free path

In the preceding sections, it is shown that $Cd_2Re_2O_7$ can be, to a good approximation, treated as the Einstein oscillators (Cd ions) embedded in a Debye host. In this section we apply this scheme to interpret the behavior of the lattice thermal conductivity (Fig. 4). An estimation of the phonon mean-free path is presented by applying the kinetic-theory relation

$$\kappa_{latt} = \frac{1}{3} C_v^l \langle v \rangle l_{ph}, \tag{5}$$

where C_v^l is the lattice specific heat per unit volume, $\langle v \rangle$ the average sound velocity, and l_{ph} the mean-free path of the heat-carrying phonons.[36] We have subtracted electronic specific heat γT from C_p. Here we apply the simple relationship of a cubic lattice

$$\langle v \rangle = \sqrt{\frac{\eta}{\rho_m}} \quad \text{with} \quad \eta = \frac{(C_{11} + 2C_{12})}{3}, \tag{6}$$

where η is the bulk modulus, C_{11} and C_{12} the elastic moduli tensors, respectively. The C_{11}, C_{12}, and C_{44} values derived in the resonant ultrasonic spectroscopy measurements[12] yield a nearly temperature independent $\langle v \rangle \sim 4.35 \times 10^3$ m s^{-1} below 300 K: the relative change with temperature is only a few percent. To facilitate the calculation, we hereafter assume a constant value of $\langle v \rangle$ in the entire temperature range studied.

With κ_{latt}, C_v^l and $\langle v \rangle$ known, l_{ph} has been calculated using Eq. (5) and subsequently plotted in Fig. 7. In contrast to the largely amorphouslike temperature dependence of κ_{latt}, the temperature dependence of l_{ph} is overall crystal-like. With increasing temperatures, l_{ph} no longer decreases above ~160 K and it forms a broad hump centered at ~340 K. In the light of Eq. (5), it is the increment of C_v^l that compensates the change in l_{ph} and gives rise to the "$d\kappa_{\text{latt}}/dT \geq 0$" feature. Finally l_{ph} reaches the value ~6 Å at 720 K. Should the bipolar effect have been taken into account, this value will be closer to that of the average Cd-Cd distance than what is shown in Fig. 7. It is consistent with the argument that the Cd ions are Einstein oscillators and they strongly interact with the heat-carrying acoustic phonon modes.

With the average inter-atomic spacing and the velocity of sound known, we estimate the minimum lattice thermal conductivity, κ_{min}, based on a phenomenological model proposed by Cahill *et al.*[43] for highly disordered or amorphous materials

$$\kappa_{\text{min}} = \left(\frac{\pi}{6}\right)^{1/3} k_B n_a^{2/3} \sum_i v_i \left(\frac{T}{\theta_i}\right)^2 \int_0^{\theta_i/T} \frac{x^3 e^x}{(e^x - 1)^2} dx, \tag{7}$$

where n_a is the number of atoms per unit volume, v_i the sound velocity, and θ_i the cut-off frequency in the unit of K for polarization i. The Cahill model is in the context of a random walk between Einstein oscillators of varying sizes. Here we have a cut-off frequency $\theta_i = v_i(\hbar/k_B)(6\pi^2 n_a)^{1/3}$ ~466 K. Substituting the θ_i value into Eq. (7) yields a κ_{min} fairly close to κ_{latt} in both magnitude and temperature dependence (Fig. 8). Figure 8 self-consistently shows how amorphouslike the heat conduction is in $Cd_2Re_2O_7$.

C. Phonon-mediated electron-hole scattering

Still to be discussed are the unusual power-law resistivity behavior observed in the regime (b), and, the slope change in

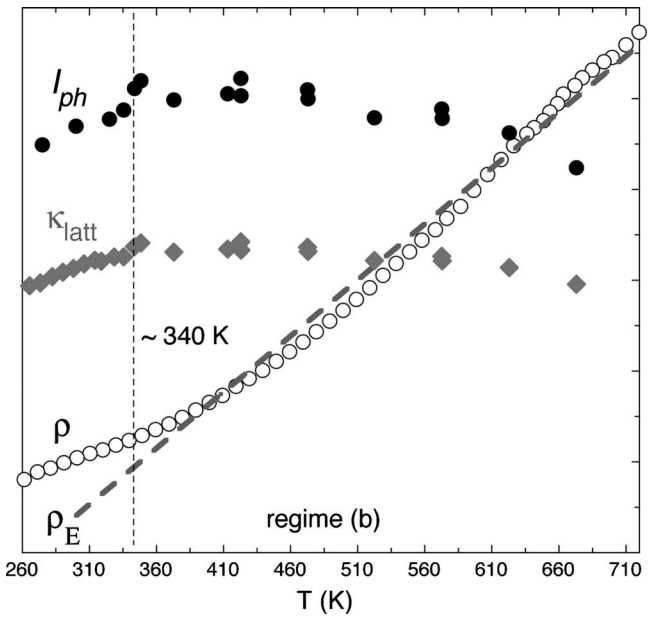

FIG. 9. Associated changes in the resistivity ρ, lattice thermal conductivity κ_{latt}, and phonon mean free path l_{ph} in the vicinity of 340 K and above. The expected resistivity contribution from Einstein oscillators ρ_E is shown, provided $\theta_E \sim 100$ K and the parameter (KN/m) $\sim 1.02 \times 10^{-3}$ Ω cm K, which achieves the best fitting over the regime (b).

thermal conductivity. At first glance, the fact that the power-law behavior is sustained well above θ_D (i.e., the characteristic energy of the acoustic phonon modes) suggests a contribution, at least partially, from the optical phonon modes. Cook proposed that the local mode contribution to the resistivity, ρ_E, could be expressed as[44]

$$\rho_E = \frac{KN}{mT(e^{\theta_E/T} - 1)(1 - e^{-\theta_E/T})}, \tag{8}$$

where m is the atomic mass, N the number of oscillators per unit volume, and K a constant that depends on the electron density and electron-local-mode coupling strength. As is clearly shown in Fig. 9, however, Eq. (8) alone is inadequate to account for the nonlinearity of the resistivity. In addition, the line shape of the high-frequency Raman peaks of $Cd_2Re_2O_7$ is fairly symmetric, consistent with a weak electron-phonon coupling.[35,36] The results of the pressure dependence studies also corroborated a rigid lattice to which electrons couple only weakly above T^*.[11,33]

At this point, it is instructive to refer to TiS_2, which exhibits a power-law resistivity behavior in the range well above room temperature.[45–48] Thompson proposed that the electron-electron scattering mechanism could dominate the electron-phonon interaction at high temperatures if "E_F is small," and it yields a T^2-dependent resistivity in TiS_2.[45] Kukkonen *et al.*[46] studied the case of electron-hole scattering in a degenerate semimetal system and confirmed the T^2 characteristics. Klipstein *et al.*[47] and Imai *et al.*[48] later attributed the observed power-law resistivity behavior in TiS_2 to the nearly equal contributions from the intravalley and intervalley scattering assisted by phonons. The values of the power-law exponent vary from 1.7 to 2.3, depending on the carrier concentration and the ratio between the intervalley and intravalley scatterings.

Return to $Cd_2Re_2O_7$, the results of band-structure calculations and magnetoresistance studies corroborated a low carrier concentration on the order of $\sim 10^{20}$ cm^{-3}, which corresponds to a "small" E_F.[32,33] As is shown in Fig. 9, the onset of the power law resistivity behavior is close to where the thermal conductivity undergoes the slope change in absence of a phase transition. This strongly suggests that these changes stem from a unifying scattering mechanism: a phonon-mediated electron-hole scattering mechanism. The electron-hole scattering, synonymous with the interband scattering in $Cd_2Re_2O_7$, is a resistive mechanism that is momentum-wise compensated by phonons. This mechanism alters the electrical and thermal transport behavior only at high temperatures, as it requires phonons with adequately large wave vectors. On the other hand, the Umklapp processes of electron-electron and hole-hole, the other processes in the case of the intraband scattering that can give rise to the resistance, are less accessible because the low carrier concentration takes up a small fraction of the space in the Brillouin zone.

IV. SUMMARY

The combined results of specific-heat, thermal-conductivity measurements, and the crystallographic data identify the Cd ions as Einstein oscillators embedded in a Debye host. $Cd_2Re_2O_7$ possesses low-frequency optical phonon modes that are strongly coupled to the acoustic phonons. As such, the system exhibits an amorphouslike lattice thermal conductivity. On the other hand, a phonon-mediated electron-hole scattering mechanism sets in above room temperature, giving rise to the power-law resistivity behavior and the slope change in the thermal conductivity at ~ 340 K.

ACKNOWLEDGMENTS

The authors are grateful to R. Jin, D. G. Mandrus, and B. C. Sales of Oak Ridge National Laboratory for many stimulating discussions. The work at Clemson University was supported by DOE/EPSCoR Implementation under Grant No. DE-FG02-04ER-46139.

*Author to whom correspondence should be addressed; jianhe@clemson.edu

[1] M. Hanawa, Y. Muraoka, T. Tayama, T. Sakakibara, J. Yamaura, and Z. Hiroi, Phys. Rev. Lett. **87**, 187001 (2001).

[2] R. Jin, J. He, S. McCall, C. S. Alexander, F. Drymiotis and D. Mandrus, Phys. Rev. B **64**, 180503(R) (2001).

[3] H. Sakai, K. Yoshimura, H. Ohno, H. Kato, S. Kambe, R. E. Walstedt, T. D. Matsuda, Y. Haga, and Y. Onuki, J. Phys.: Condens. Matter **13**, L785 (2001).

[4] P. C. Donohue, J. M. Longo, R. D. Rosenstein, and L. Katz, Inorg. Chem. **4**, 1152 (1965).

[5] K. Blacklock and H. W. White, J. Chem. Phys. **71**, 5287 (1979).

[6] M. D. Lumsden, S. R. Dunsiger, J. E. Sonier, R. I. Miller, R. F. Kiefl, R. Jin, J. He, D. Mandrus, S. T. Bramwell, and J. S. Gardner, Phys. Rev. Lett. **89**, 147002 (2002).

[7] R. Kadono, W. Higemoto, A. Koda, Y. Kawasaki, M. Hanawa, and Z. Hiroi, J. Phys. Soc. Jpn. **71**, 709 (2002).

[8] Z. Hiroi, J. Yamaura, Y. Muraoka, and M. Hanawa, J. Phys. Soc. Jpn. **71**, 1634 (2002).

[9] C. Lu, J. Zhang, R. Jin, H. Qu, J. He, D. Mandrus, K.-D. Tseng, C.-T. Tzeng, L.-C. Lin, and E. W. Plummer, Phys. Rev. B **70**, 092506 (2004).

[10] R. Jin, J. He, J. R. Thompson, M. F. Chisholm, B. C. Sales, and D. Mandrus, J. Phys.: Condens. Matter **14**, L117 (2002).

[11] N. Barišić, L. Forro, D. Mandrus, R. Jin, J. He, and P. Fazekas, Phys. Rev. B **67**, 245112 (2003).

[12] I. Sergienko, V. Keppens, M. McGuire, R. Jin, J. He, S. Curnoe, B. Sales, P. Blaha, D. Singh, K. Schwarz, and D. Mandrus, Phys. Rev. Lett. **92**, 065501 (2004).

[13] C. A. Kendziora, I. A. Sergienko, R. Jin, J. He, V. Keppens, B. C. Sales, and D. Mandrus, Phys. Rev. Lett. **95**, 125503 (2005).

[14] J. Yamaura and Z. Hiroi, J. Phys. Soc. Jpn. **71**, 2598 (2002).

[15] O. Vyaselev, K. Arai, K. Kobayashi, J. Yamazaki, K. Kodama, M. Takigawa, M. Hanawa, and Z. Hiroi, Phys. Rev. Lett. **89**, 017001 (2002).

[16] J. He, R. Jin, B. Chakoumakos, J. Gardner, D. Mandrus, and Terry M. Tritt, J. Electron. Mater. **36**, 740 (2007).

[17] J. P. Castellan, B. D. Gaulin, J. van Duijn, M. J. Lewis, M. D. Lumsden, R. Jin, J. He, S. E. Nagler, and D. Mandrus, Phys. Rev. B **66**, 134528 (2002).

[18] J. C. Petersen, M. D. Caswell, J. S. Dodge, I. A. Sergienko, J. He, R. Jin, and D. Mandrus, Nat. Phys. **2**, 605 (2006).

[19] ^{114}Cd is the most neutron scattering friendly isotope of Cadmium. The time-of-flight spectrum taken on an isotope-enriched (^{114}Cd, $>98.5\%$) specimen was severely degraded by the strongly resonating absorption between wavelength 0.5 and 2.0 Å.

[20] M. A. Subramanian, G. Aravamudan, and G. V. Subba Rao, Prog. Solid State Chem. **15**, 55 (1983).

[21] J. He, Ph.D. thesis, the University of Tennessee, 2004.

[22] C. S. Knee, J. Holmlund, J. Andreasson, M. Käll, S. G. Eriksson, and L. Börjesson, Phys. Rev. B **71**, 214518 (2005).

[23] H. Sakai, H. Kato, S. Kambe, R. E. Walstedt, H. Ohno, M. Kato, K. Yoshimura, and H. Matsuhata, Phys. Rev. B **66**, 100509(R) (2002).

[24] For example, L. Klein, J. S. Dodge, C. H. Ahn, J. W. Reiner, L. Mieville, T. H. Geballe, M. R. Beasley, and A. Kapitulnik, J. Phys.: Condens. Matter **8**, 10111 (1996).

[25] D. Mandrus, J. R. Thompson, R. Gaál, L. Forró, J. C. Bryan, B. C. Chakoumakos, L. M. Woods, B. C. Sales, R. S. Fishman, and V. Keppens, Phys. Rev. B **63**, 195104 (2001).

[26] I. Kézsmárki, N. Hanasaki, D. Hashimoto, S. Iguchi, Y. Taguchi, S. Miyasaka, and Y. Tokura, Phys. Rev. Lett. **93**, 266401 (2004).

[27] R. E. Carbonio, J. A. Alonso, and J. L. Martinez, J. Phys.: Condens. Matter **11**, 361 (1999).

[28] For example, N. W. Ashcroft and N. D. Mermin, *Solid State Physics* (Saunders, Philadelphia, 1976).

[29] V. Ponnambalam, S. Lindsey, N. S. Hickman, and Terry M. Tritt, Rev. Sci. Instrum. **77**, 073904 (2006).

[30] B. M. Zawilski, R. T. Littleton IV, and T. M. Tritt, Rev. Sci. Instrum. **72**, 1770 (2001).

[31] J. Merino and R. H. McKenzie, Phys. Rev. B **61**, 7996 (2000).

[32] D. J. Singh, P. Blaha, K. Schwarz, and J. O. Sofo, Phys. Rev. B **65**, 155109 (2002).

[33] Z. Hiroi, T. Yamauchi, T. Yamada, M. Hanawa, Y. Oshishi, O. Shimomura, M. Abliz, M. Hedo, and Y. Uwatoko, J. Phys. Soc. Jpn. **71**, 1553 (2002); Z. Hiroi, M. Hanawa, Y. Muraoka, and H. Harima, *ibid.* **72**, 21 (2003).

[34] We haven't found any magnetic field dependence of the magnetic susceptibility, resistivity, thermopower, and thermal conductivity in the experimentally accessible range. The lack of a magnetic field dependence of thermopower below 300 K has been formerly reported by D. Huo, A. Mitsuda, Y. Isikawa, J. Sakurai, H. Sakai, H. Ohno, M. Kato, K. Yoshimura, S. Kambe, and R. E. Walstedt, J. Phys.: Condens. Matter **14**, L257 (2002).

[35] The low carrier mobility restricted us from extracting the lattice thermal conductivity by applying a transverse magnetic field.

[36] For example, *Thermal Conductivity: Theory, Properties, and Applications*, Edited By Terry M. Tritt (Kluwer Academic/Plenum Publishers, New York, 2004).

[37] J. L. Cohn, G. S. Nolas, V. Fessatidis, T. H. Metcalf, and G. A. Slack, Phys. Rev. Lett. **82**, 779 (1999).

[38] B. C. Sales, B. C. Chakoumakos, D. Mandrus, and J. W. Sharp, J. Solid State Chem. **146**, 528 (1999). Here we neglect the possible static disorder of Cd ions and only use the room temperature U_{iso} value to extrapolate the slope to the origin, the error is usually $<10\%$ when the Debye temperature <600 K.

[39] It is the isochoric specific heat C_V that approaches the Dulong-Petit limit. Nonetheless, it doesn't alter the conclusion as one always has $C_v \leq C_p$.

[40] R. K. Crawford, W. F. Lewis, and W. B. Daniels, J. Phys. C **9**, 1381 (1976).

[41] R. G. Ross, Phys. Chem. Liq. **23**, 189 (1991).

[42] For example, H. M. Rosenberg, *The Solid State* (Clarendon, Oxford, 1978), Chap. 6.

[43] D. G. Cahill, S. K. Watson, and R. O. Pohl, Phys. Rev. B **46**, 6131 (1992).

[44] J. R. Cooper, Phys. Rev. B **9**, 2778 (1974).

[45] A. H. Thompson, Phys. Rev. Lett. **35**, 1786 (1975).

[46] C. A. Kukkonen and P. F. Maldague, Phys. Rev. Lett. **37**, 782 (1976).

[47] P. C. Klipstein, A. G. Bagnall, W. Y. Liang, E. A. Marseglia, and R. H. Friend, J. Phys. C **14**, 4067 (1981).

[48] H. Imai, Y. Shimakawa and Y. Kubo, Phys. Rev. B **64**, 241104(R) (2001).